Available online at www.sciencedirect.com
SCIENCE DIRECT®
Journal of Solid State Chemistry 177 (2004) 1365–1371
JOURNAL OF SOLID STATE CHEMISTRY
http://elsevier.com/locate/jssc

Study on ESR and inter-related properties of vacuum-dehydrated nanotubed titanic acid

Shunli Zhang, Wei Li, Zhensheng Jin,* Jianjun Yang, Jingwei Zhang, Zuliang Du, and Zhijun Zhang*

Laboratory of Special Functional Materials, Henan University, Kaifeng 475001, China

Received 23 July 2003; received in revised form 3 November 2003; accepted 23 November 2003

Abstract

Nanotubed titanic acid ($H_2Ti_2O_4(OH)_2$) is a novel kind of material. The electron spin resonance (ESR) and inter-related properties of its vacuum-dehydrated product were investigated by means of transmission electron microscopic, X-ray diffraction, ESR, diffuse reflectance spectra. The results showed that after treatment under vacuum (−0.1 MPa) at 100°C, single-electron-trapped oxygen vacancies (SETOV), characterized by a symmetrical ESR signal ($g = 2.003$), were generated in nanotubed $H_2Ti_2O_4(OH)_2$ crystal lattice. The $g = 2.003$ ESR signal intensity (I_{ESR}) increased with treatment time. SETOV played the role of F centers, the visible-light absorption power of vacuum-dehydrated $H_2Ti_2O_4(OH)_2$ was proportional to I_{ESR}. During vacuum dehydration at 100°C, the $H_2Ti_2O_4(OH)_2$ nanotubes shortened but its crystalline form kept unchanged. The formation mechanism of SETOV was discussed.

Keywords: Nanotubed titanic acid; ESR

1. Introduction

Titanic acids with different compositions and morphologies can be prepared from the corresponding alkaline metal (Na, K, etc.) titanates. Immersing in a 0.5 M HCl solution at 60°C, zigzag structured $Na_2Ti_3O_7$ was completely hydrolyzed to $H_2Ti_3O_7$ [1,2]. In a 0.1 M HCl solution, needle-shaped $Na_4Ti_9O_{20} \cdot xH_2O$ was converted into $H_4Ti_9O_{20} \cdot xH_2O$; $H_4Ti_9O_{20} \cdot xH_2O$ can be thermally decomposed to TiO_2 at 700°C [3]. A layered $H_2Ti_4O_9 \cdot 1.2H_2O$ was obtained by extracting the interlayered K^+ ions of $K_2Ti_4O_9$ with a 1 M HCl solution [4]. Layered $H_2Ti_2O_5{-}2.2H_2O$, which has a C-base-centered orthorhombic structure with the lattice constant $a_0 = 18.08 \pm 0.03$ Å, $b_0 = 3.784 \pm 0.003$ Å and $c_0 = 2.998 \pm 0.002$ Å, was prepared by percolation of 0.01 M HNO_3 as an eluent through a column packed with the $(Li_{1.81}H_{0.19})Ti_2O_5{-}2.2H_2O$ [5]. In 1998, by treating anatase TiO_2 powder with a 5–10 M NaOH aqueous solution at 110°C for 20 h, Kasuga et al. [6] obtained a nanotubed material (Jin et al. [7] repeated their work in 2000). This nanotubed material was determined to be $Na_2Ti_2O_4(OH)_2$, which in a pH 1 HCl solution can be converted to nanotubed $H_2Ti_2O_4(OH)_2$ [8,9].

Nanotubed $H_2Ti_2O_4(OH)_2$ is a novel kind of titanic acid, the studies of its physico-chemical properties and functions are systematically in progress in our laboratory, e.g., the influence of annealing temperature on its morphology, structure and photocatalytic activity as well as the visible photoluminescence property [10–12], especially the visible-light absorbtion property of its vacuum-dehydrated product (because the visible-light absorbtion property may be applicable in visible-light photocatalysis). The results and discussion about the electron spin resonance (ESR) and inter-related properties of vacuum-dehydrated nanotubed titanic acid are reported in this paper.

2. Experimental section

2.1. Preparation of samples [8,9]

About 300 mL of 40% (w/w) NaOH aqueous solution was put into a PTFE bottle (equipped with a reflux

*Corresponding authors. Fax: +86-378-2867282.
E-mail address: zhenshengjin@henu.edu.cn (Z. Jin).

0022-4596/$ - see front matter © 2003 Elsevier Inc. All rights reserved.
doi:10.1016/j.jssc.2003.11.027

condenser) which was placed in an oil bath. After the temperature of NaOH solution reached 110°C, 6 g raw TiO_2 powder was added and the mixture was magnetically stirred during 20 h, then the reaction was cut out. The dispersion, being cooled to room temperature, was diluted with deionized water to a pH of ca. 13. The solid settled from the dispersion was divided in two aliquots. Sample 1 was obtained by washing the first aliquot with anhydrous ethanol to remove free NaOH adsorbed on both the outside and inside surfaces, then it was filtered and dried at room temperature. Sample 2 was prepared by washing the other aliquot with deionized water to a pH of 7–8 and immersing it in a pH 1 HCl solution. This solution was magnetically stirred during 5 h, washed again with deionized water to remove Cl^-, and dried under vacuum at room temperature to remove the adsorbed water. According to the contents of Na, Ti and structural water determined, sample 1 was $Na_2Ti_2O_4(OH)_2$(Na/Ti atomic ratio = 1), and sample 2 chemical formula was $H_2Ti_2O_4(OH)_2$(Na/Ti atomic ratio = 0, H_2O/TiO_2 mole ratio close to 1). Four aliquots of sample 2 accurately weighed were treated under vacuum (−0.1 MPa) at 100°C for 2, 8, 23, 48 h, respectively; the weight loss in % was then measured at different treatment times.

2.2. Na, Ti analysis and structural water determination

Ti contents of samples 1 and 2 were determined by means of colorimetric method (Ti^{4+} and H_2O_2 can form an orange-yellowish complex in H_2SO_4 solution), a UNICAM λ HE10S α UV–Vis absorption spectrometer was used for this analysis. Na contents were analyzed using a Hitachi 180-60 atomic absorption spectrometer. The structural water of sample 2 was measured according to the following procedure: a crucible containing an accurately weighed amount of sample 2 was put in a muffle furnace, temperature was slowly raised to 700°C in air ambience and kept constant during 4 h. The sample was weighed immediately after its cooling to room temperature. The weight lost was directly related to the structural water of sample 2.

2.3. Characterization

ESR spectra (first derivative of absorption curve) were recorded under dark at room temperature using a Brüker ESP 300E spectrometer which was operated in the X band(ca. 9.80 GHz) with 100 kHz field modulation, 0.2 mT amplitude modulation and 10 mW microwave power. Sweep time was 41.9 s. The g values were measured by taking $g = 2.0036$ of diphenyl picryl hydrazyl as reference. Transmission electron microscopic (TEM) pictures were obtained using a JEM-2010 electron microscope. X-ray diffraction (XRD) patterns were measured on a Philips X'Pert Pro X-ray diffractometer. UV–Vis diffuse reflectance spectra (DRS) were recorded on a Shimadzu U-3010 spectrometer.

2.4. Reagents

NaOH, analytically pure, a product of Tianjin Chemical Reagents Factory; HCl, analytically pure, a product of Kaifeng Chemical Reagents Factory; Raw TiO_2 (anatase) was purchased from Jiangsu Hehai Nano Sci-Tech Company; anhydrous ethanol, analytically pure, was produced by Tianjin Hongyan Reagents Factory.

3. Results

The morphology of nanotubed $H_2Ti_2O_4(OH)_2$ is shown in Fig. 1(a). Lots of nanotubes consist of 2–8

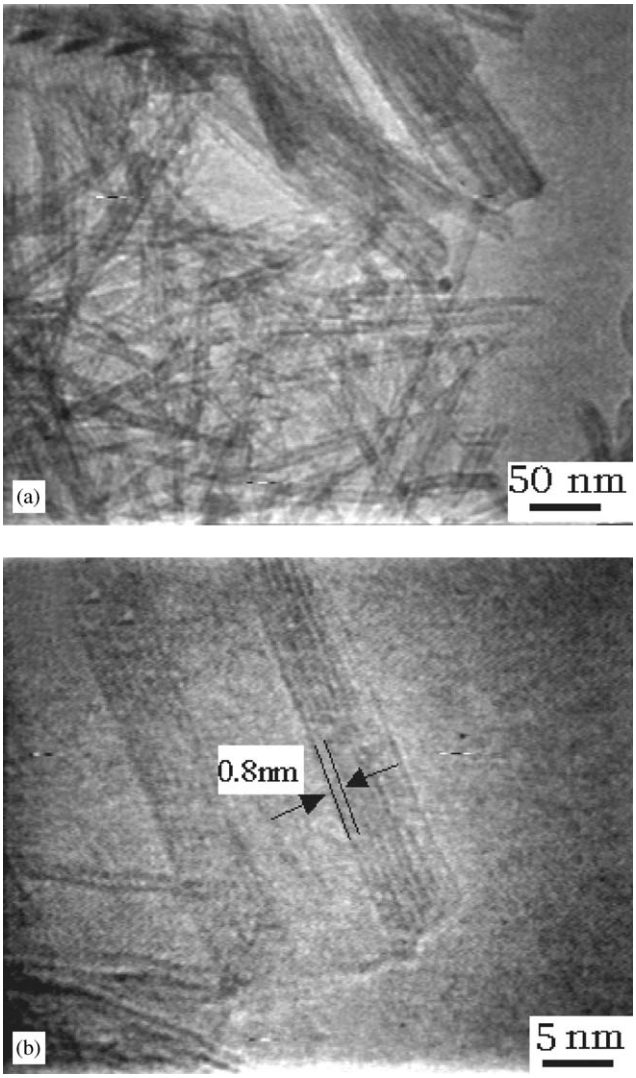

Fig. 1. TEM pictures of nanotubed $H_2Ti_2O_4(OH)_2$: (a) lots of nanotubes, and (b) an eight-layered nanotube.

layers, Fig. 1(b) is a typical eight-layered nanotube of $H_2Ti_2O_4(OH)_2$ with inner and outer diameters ca. 6.4 and 18.6 nm, respectively, distance between two adjacent layers ca. 0.8 nm. XRD patterns in Fig. 2 show that the crystalline form of nanotubed $H_2Ti_2O_4(OH)_2$ is similar to that of nanotubed $Na_2Ti_2O_4(OH)$ (Table 1, $a_0 = 19.26$ Å, $b_0 = 3.78$ Å) and belongs to an orthorhombic system (insert is a hypothetical view of $X-Y$ section) [5,13]. Since the layers of nanotubed $Na_2Ti_2O_4(OH)$ and $H_2Ti_2O_4(OH)_2$ are curved, their lattice constant a_0 is different from that of flat layered $Li_{1.81}H_{0.19}Ti_2O_5 \cdot 2.2H_2O$ ($a_0 = 16.66$ Å) [5] and $H_2Ti_2O_5 \cdot H_2O$ ($a_0 = 18.08$ Å) [13]. After heating the sample to 100°C under vacuum (−0.1 MPa), the following properties were observed for the dehydrated nanotubed $H_2Ti_2O_4(OH)_2$:

(i) Weight loss increases with treatment duration (Fig. 3), at $t \approx 50$ h the sample weight reaches constant.
(ii) Dehydrated product exhibited a symmetrical ESR signal centered at $g = 2.003$ (Fig. 4(a)). The curve of the relation between ESR signal intensity (I_{ESR})

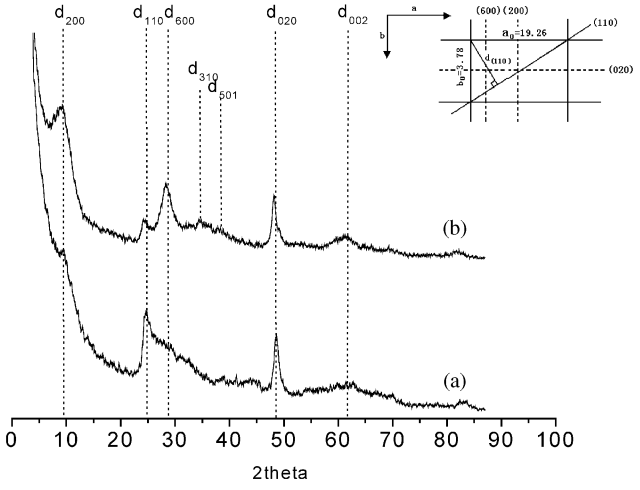

Fig. 2. XRD patterns: (a) nanotubed $H_2Ti_2O_4(OH)_2$, and (b) nanotubed $Na_2Ti_2O_4(OH)_2$. (Inset: a hypothetical schematic view of $X-Y$ section of orthorhombic crystal form).

Table 1
Diffraction data of nanotubed $Na_2Ti_2O_4(OH)_2$

2θ	d (Å)[a]	$h\,k\,l$	I/I_0	Remarks
9.18	9.63	200	100	d_{200} approximately equals to the distance between adjacent layers of multilayered nanotube
24.30	3.66	110	32	
28.14	3.17	600	60	
34.24	2.62(?)	301	8	
38.06	2.36(?)	501	10	
48.14	1.89	020	69	
61.76	1.50(?)	002	8	

[a] Lattice parameter: $a_0 = 19.26$ Å, $b_0 = 3.78$ Å.

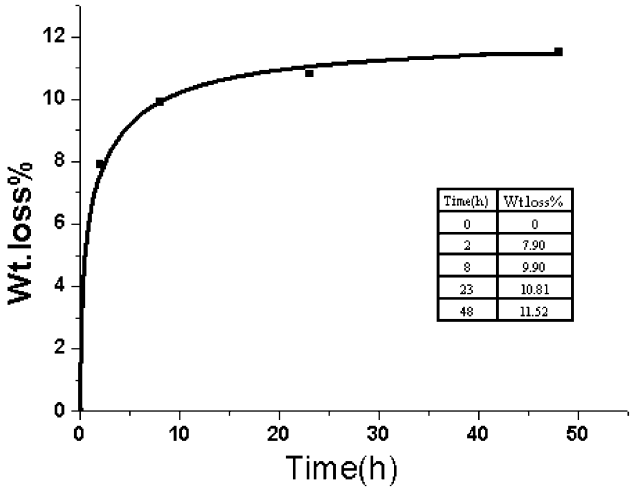

Fig. 3. Dependence of weight loss % on vacuum-dehydration time at 100°C for nanotubed $H_2Ti_2O_4(OH)_2$.

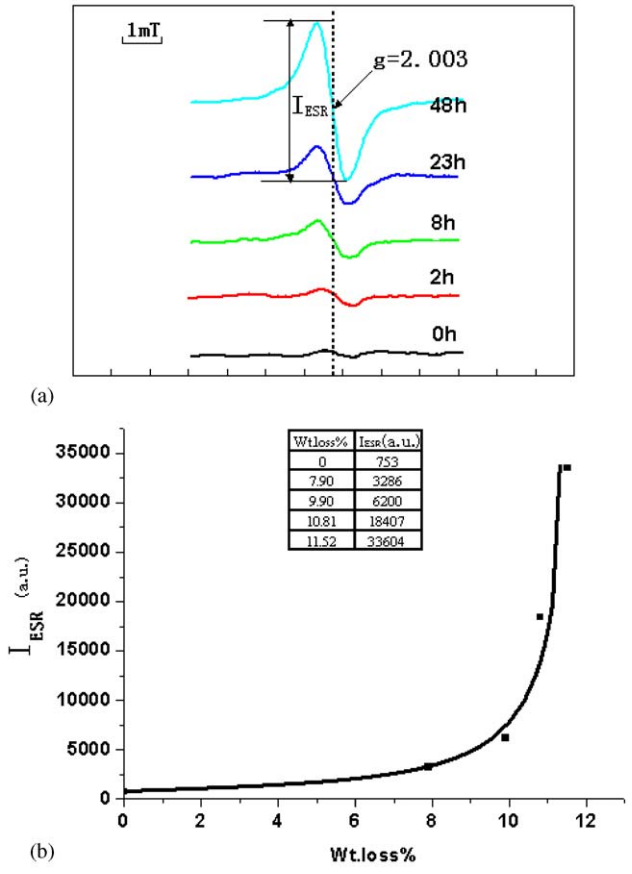

Fig. 4. Relation between I_{ESR} ($g = 2.003$) and vacuum-dehydration time (t) at 100°C for nanotubed $H_2Ti_2O_4(OH)_2$: (a) ESR signals at different vacuum-dehydration times, and (b) $I_{ESR}-t$ curve.

was plotted as a function of weight loss in percent (wt. loss%) is shown in Fig. 4(b). As the sample weight reaches constant, the enhancement of ESR signal intensity also ceases. The as-prepared sample

dried at room temperature possesses a small amount of single-electron-trapped oxygen vacancies (SETOV) ($I_{ESR} = 753$ a.u.) (Fig. 4(b)).

(iii) Nanotubes break, the longer the duration was, the shorter the nanotubes were (Fig. 5(a)), while XRD patterns (Fig. 5(b)) show that peak (200) width increased and that its position shifted to higher value of 2θ when the treatment was prolonged. Peaks (110) (600) (020) remained unchanged.

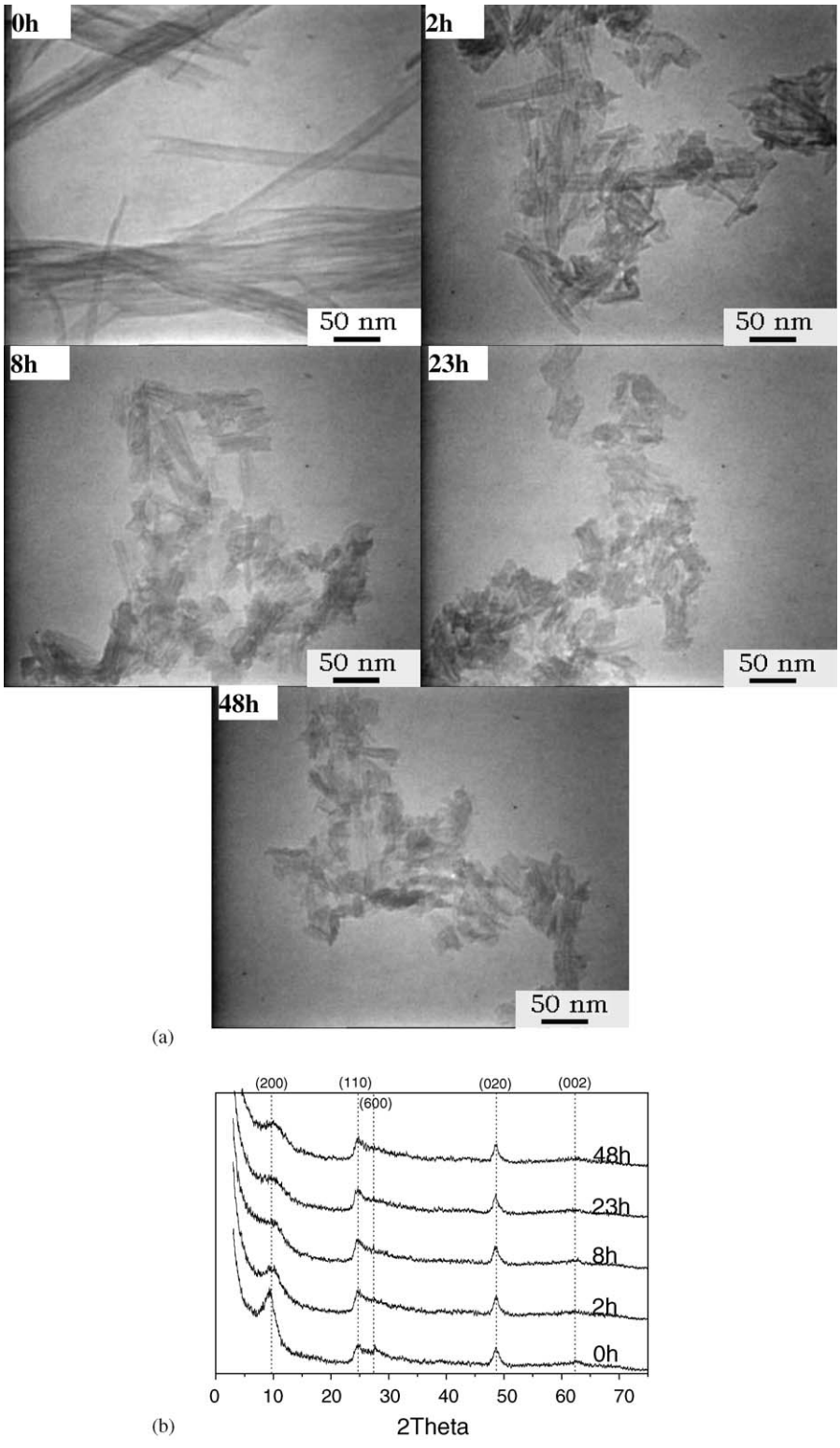

Fig. 5. TEM pictures (a), and XRD patterns (b) of nanotubed $H_2Ti_2O_4(OH)_2$ vacuum-dehydrated at different times.

(iv) Comparing with raw TiO_2 (anatase), dehydrated products have a broad absorption at $\lambda > 400$ nm (Fig. 6(a)). The curve of the relation between R'_∞ and I_{ESR} is shown in Fig. 6(b), where R'_∞ represents the reflectance determined at $\lambda = 450$ nm, $R'_\infty = R_\infty(\text{sample})/R_\infty(\text{reference substance } BaSO_4)$.

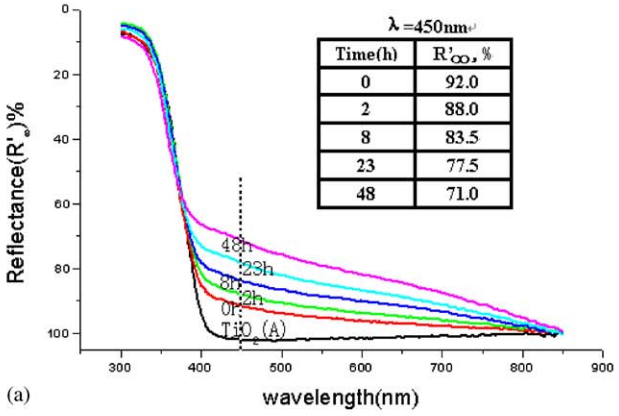

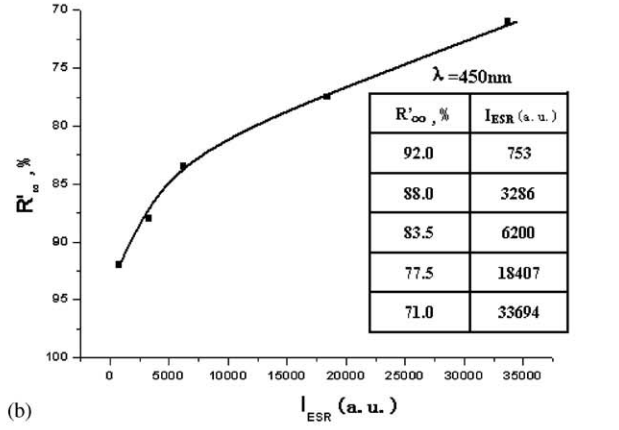

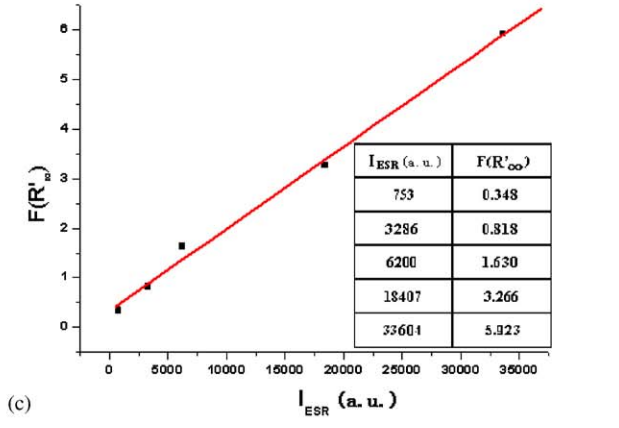

Fig. 6. Change of DRS spectra of nanotubed $H_2Ti_2O_4(OH)_2$ with vacuum-dehydration times at 100°C: (a) DRS spectra, (b) $R'_\infty - I_{ESR}$ curve, and (c) $F(R'_\infty) - I_{ESR}$ straight line.

4. Discussion

It was known that electron-trapped oxygen vacancies (characterized by a $g = 2.003$ ESR signal) and Ti^{3+} ions (characterized by a $g = 1.96$ ESR signal) are generated in TiO_2 crystal lattice by heating under high vacuum [14,15,17] or reducing in hydrogen atmosphere [16]. However, such oxygen vacancies and Ti^{3+} ions are unstable in room atmosphere. Using discharge of radio waves to treat TiO_2(anatase) under 2 Torr H_2 at 673 K, Nakamura et al. [18] did not detect electron-trapped oxygen vacancies in TiO_2(anatase). A $g = 2.004$ ESR signal appeared only under visible light illumination, did not appear under dark. Fig. 4(a) shows the ESR spectra (measured under dark) of the vacuum-treated nanotubed titanic acid, no $g = 1.96$ ESR signal of Ti^{3+} ions was found. Referring to literature [14,15,18], this symmetrical ESR signal ($g = 2.003$) was attributed to the SETOV. These SETOV are stable in air. Figs. 3 and 4(b) underline the influence of dehydration on SETOV creation in nanotubed $H_2Ti_2O_4(OH)_2$.

How to explain the results shown in Figs. 3–5? The structure of TiO_2(anatase) can be described in terms of chains of distorted TiO_6 octahedra [19,20]. Each Ti^{4+} is surrounded by an octahedron of six O^{2-} ions. Two Ti–O bonds are longer (1.980 Å) and thus weaker than the four others (1.934 Å). The coordination number of O^{2-} with Ti^{4+} is three. According to HRTEM study on the formation process of nanotubed $Na_2Ti_2O_4(OH)_2$ [12,9], we assumed that treating TiO_2(anatase) with concentrated NaOH solution induced preferentially the rupture of the longer Ti–O bonds due to OH^- ions action (Fig. 7a) [9]. Then, linear fragments are formed and peel off from the TiO_2 crystalline particles. The linear fragments are linked together by O^-–Na^+–O^- ionic bonds and thus form planar fragments. The $(–Ti–O–Ti–O–Ti–O–)_x$ chains included in planar fragments are flexible by the covalent link between their end groups, and they can form the thermodynamically stable product, i.e., solid nanotubed $Na_2Ti_2O_4(OH)_2$ could be obtained; the monolayer nanotube may thus play the role of the template for multilayer nanotube. Such a formation process of nanotubed $Na_2Ti_2O_4(OH)_2$ is depicted by Fig. 7a [9]. After replacing of Na^+ with H^+ using a pH 1 HCl solution, the intralayer composition of nanotubed $H_2Ti_2O_4(OH)_2$ can be described by Fig. 7b. In this model, there are two possible ways of losing the first water molecule. Way I will leave a hydrogen vacancy (V'_H, with an effective charge -1) and an SETOV ($V^{\bullet}_O$, with an effective charge $+1$), here the oxygen vacancy trapped one electron is the requirement of charge neutrality. According the principle of charge neutrality the reaction formula is expressed as follows:

$$2OH \rightarrow H_2O + V'_H + V^{\bullet}_O.$$

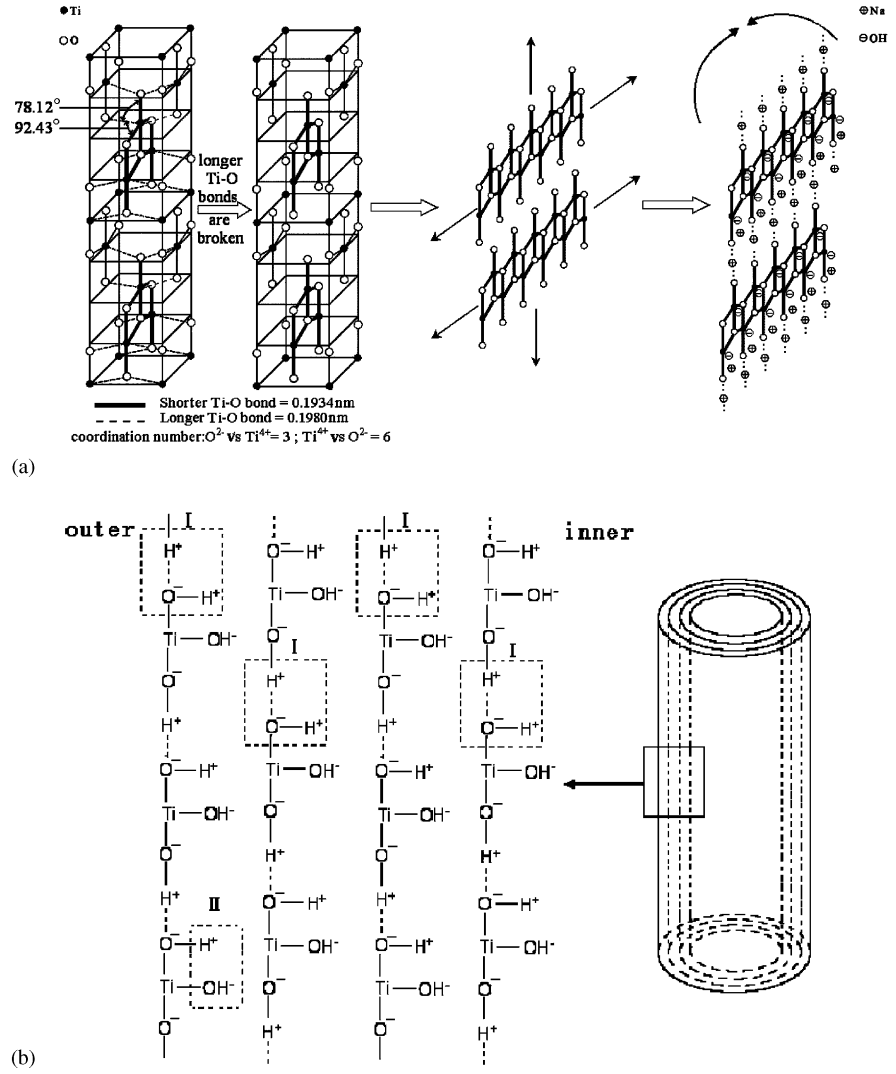

Fig. 7. Schematic diagrams: (a) formation process of nanotubed $Na_2Ti_2O_4(OH)_2$, and (b) mechanism for breaking of $H_2Ti_2O_4(OH)_2$ nanotube.

This route could induce the breaking of the nanotube as the dehydration takes place in the vicinity of a cross-section, while way II could not. Due to the larger spacing (ca. 0.8 nm), the losing of the first water molecule between two adjacent layers seems to be impossible. So, under vacuum at 100°C, way I will be the main dehydration route ($H_2Ti_2O_4(OH)_2 \rightarrow H_{2(1-x)}Ti_2O_{4-x}(OH)_2 + xH_2O + xV_O^{\bullet} + xV_H'$); if the treatment is not stopped, the length of nanotubes will be increasingly short (Fig. 5(a)). Although the shape and position of peak (200) slightly change, the orthorhombic crystalline form keeps unchanged (Fig. 5(b)).

It was known that the oxygen vacancy states in TiO_2 were located 2.02–2.45 eV above the valence band and this bandgap energy corresponds to the energy of visible light [16,18]. Fig. 6(b) shows that dehydrated nanotubed $H_2Ti_2O_4(OH)_2$ is also responsible to visible light and R'_∞ decreases with the enhancing of I_{ESR}. According to Kubelka–Munk (KM) theory for the diffuse reflectance of powder sample, the KM function is as follows [21,22]:

$$K/S = (1 - R_\infty)^2/2\,R_\infty = F(R_\infty), \quad (1)$$

where constants K and S characterize the losses of incident light due to absorption and scattering, respectively. Since S is independent of wavelength, so $F(R_\infty)$ is proportional to the real absorption power of sample:

$$F(R_\infty) = (1 - R_\infty)^2/2\,R_\infty \propto \text{absorption power}. \quad (2)$$

Replacing R_∞ by R'_∞,

$$F(R'_\infty) = (1 - R'_\infty)^2/2R'_\infty \propto \text{absorption power}. \quad (3)$$

The concentration of SETOV (C_{SETOV}) is proportional to I_{ESR}. If SETOV plays the role of F centers, then

$$F(R'_\infty) = (1 - R'_\infty)^2/2\,R'_\infty \propto C_{SETOV} \propto I_{ESR}. \quad (4)$$

The plot of $(1-R'_\infty)^2/2R'_\infty$ as a function of I_{ESR} gives a straight line (Fig. 6(c)) which underlines the direct correlation between I_{ESR} and $F(R'_\infty)$ and confirmed that the hypothesis of a relation between R'_∞ and I_{ESR} is reasonable.

If the e^-–h^+ pairs generated from intrabandgap transition were separated and transferred to solid surface, this visible-light absorption property of vacuum-dehydrated nanotubed $H_2Ti_2O_4(OH)_2$ may be applied in visible-light photocatalysis. Now it is under investigation in our laboratory.

5. Conclusions

Under vacuum at 100°C, nanotubed $H_2Ti_2O_4(OH)_2$ can be dehydrated to generate SETOV in its crystal lattice, which are demonstrated by ESR signal ($g = 2.003$). The concentration of SETOV (C_{SETOV}) is proportional to I_{ESR} and plays the role of F centers, so the visible-light absorption is proportional to I_{ESR}. In the course of dehydration, $H_2Ti_2O_4(OH)_2$ nanotubes break; longer the treating time, shorter the length of nanotube, but its crystalline form keeps unchanged.

Acknowledgments

This work is supported by National Natural Science Foundation of China (No. 20071010). The authors are indebted to Prof. Chen Jingrong's help for the measurements and discussion of ESR data.

References

[1] H. Izawa, S. Kikkawa, M. Koizymi, J. Phys. Chem. 86 (1982) 5023–5026.
[2] H. Izawa, S. Kikkawa, M. Koizymi, J. Solid State Chem. 60 (1985) 264–267.
[3] A. Clearfield, J. Lehto, Preparation, J. Solid State Chem. 73 (1988) 98–106.
[4] T. Sasaki, M. Watanabe, Y. Komatsu, Y. Fujiki, Inorg. Chem. 24 (1985) 2265–2271.
[5] M. Sugita, M. Tsuji, M. Abe, Bull. Chem. Soc. Japan 63 (1990) 1978–1984.
[6] T. Kasuga, M. Hiramatsu, A. Hoson, T. Sekino, K. Niihara, Langmuir 14 (1998) 3160–3163.
[7] Sunli Zhang, Jingfang Zhou, Zhijun Zhang, A.V. Vorontsov, Zhengsheng Jin, Chin. Sci. Bull. 45(16) (2000) 1533–1536.
[8] Wang Xiao-dong, Li Wei, Yang Jian-Jun, Jin Zhen-sheng, Zhang Zhi-Jun, Chem. Res. 14 (2003) 5–8 (in Chinese).
[9] Jianjun Yang, Zhensheng Jin, Xiaodong Wang, Wei Li, Jingwei Zhang, Shunli Zhang, Xinyong Guo, Zhijun Zhang, Dalton Trans. 20 (2003) 3898–3901.
[10] Wang Xiaodong, Yang Jianjun, Yin Haoyong, Zhang Zhijun, Jin Zhensheng, Photogr. Sci. Photochem. 20 (2002) 424 (in Chinese).
[11] L. Qian, Z.S. Jin, J.W. Zhang, Y.B. Huang, Z.J. Zhang, Z.L. Du, Appl. Phys. A, in press.
[12] Jingwei Zhang, Xinyong Guo, Zhensheng Jin, Shunli Zhang, Jingfangzhou, Zhijun Zhang, Chin. Chem. Lett. 14 (2003) 419–423.
[13] Joinf Committee on Powder Diffraction Standard, 47-0124.
[14] E. Serwicka, M.W. Schlierkamp, R.N. Schindler, Z. Naturforch. 36a (1981) 226–232.
[15] E. Serwicka, Colloids Surf. 13 (1985) 287–293.
[16] D.C. Cronemeyer, Phys. Rev. 113 (1959) 1222–1226.
[17] A. Linsebigler, G. Lu, J.T. Yates Jr., J. Phys. Chem. 100 (1996) 6631–6636.
[18] I. Nakamura, N. Negishi, S. Kutsuna, T. Ihara, S. Sugihara, K. Takeuchi, J. Mol. Catal. A: Chem. 161 (2000) 205–212.
[19] J.K. Burdett, T. Hughbanks, J. Miller, J.W. Richardson, J.V. Smith, J. Am. Chem. Soc. 109 (1987) 3639.
[20] A. Fahmi, C. Minot, Phys. Rev. B 47 (1993) 11717.
[21] J.R. Anderson, K.C. Pratt, Introduction to Characterization and Testing of Catalysts, Academic Press, Australia, 1985.
[22] W.W. Wendlandt, H.G. Hecht, Reflectance Spectroscopy, Wiley Interscience, New York, 1966.